MATERIALS PHYSICS AND MECHANICS RESEARCH ARTICLE

Submitted: March 10, 2025 **Revised: October 18, 2024** **Accepted: April 17, 2025**

Elastic-plastic deformation when bending rotating workpieces

T.V. Brovman ✉

Tver State Technical University, Tver, Russia

✉ brovman@mail.ru

ABSTRACT

A method of calculating plastic deformation during bending a rotating circular beam is presented. Rotating blank loading is examined in the two cases: plastic deformation occurs over the thickness of the blank and plastic deformation is absent in the blank. When the pipe being bent rotates, the symmetry with respect to the force plane is broken. The nature of bending deformation of a rotating blank differs from that of a fixed one. Since the beam axis is not a plane but a space curve, there is a lateral displacement and deviation of the deflection from the force plane.

KEYWORDS

plastic deformation • acceleration limits • strain rate tensor

Citation: Brovman TV. Elastic-plastic deformation when bending rotating workpieces. *Materials Physics and Mechanics*. 2025;53(2): 113–122.
http://dx.doi.org/10.18149/MPM.5322025_10

Introduction

The methods used for bending circular blanks, such as bending by rotational pulling, compression, pressure, and rolling, must provide the product of high quality. The commonly used methods of bending beams on rollers ensure their bending in one plane. Bending occurs due to compressive stresses above the neutral axis and due to tensile stresses below it. The basic theory of plastic deformation of sheets and shells developed by A.A. Ilyushin, N.N. Malinin, R. Hill, etc. does not apply to the bending of rotating circular blanks as their bending belongs to the problems that are more complex. The lack of analytical solutions to these problems hinders the creation of engineering methods to calculate the deformed bending of rotating blanks, which negatively affects the quality of technological processes of pipe bending production. In addition, there is no information on theoretical and experimental research on the issue in the literature. Though S. Clifford, K. Pan, K.A. Stelson, W.C. Whang as well as V.S. Yusupov, R.L. Shatalov [1–5] et al. published their findings on displacement and deformation fields of plastic bending of a pipe under the action of torque or transverse force, their solutions cannot serve as a theoretical basis for pipe bending processes due to the simplified blank loading scheme.

PAO TMK (Pipe Metallurgical Co., OJSC), Seversky Pipe Plant, Taganrog Metallurgical Works, SMS Meer, Danieli, and Multistand Pipe Mill use the tools for alignment and bending where circular blanks move non-rotating through a cage that follows a closed trajectory. The problem of fixed pipe deformation has been well studied. The rotation of a pipe being deformed during bending is not believed to affect its deformation significantly.

The novelty of this research lies in the determination of the direction of maximum deflection during the elastic-plastic bending of rotating circular beams. The purpose and

Publisher: Peter the Great St. Petersburg Polytechnic University

objectives of the research are to develop methods of calculating deformations and stresses during this process, with rotation during bending taken into account. The purpose is achieved by solving differential equations for bending under concentrated loads. The research also aims to determine the functional dependence of the deflection direction on the bending moment value.

Object of research

This research examines the elastic-plastic deformation of circular beams that undergo small deformations and rotations. It does not take into account the curvature of beam sections, tangential stresses, or the effects of hardening as well as the Bauschinger effect.

The example of a thin-walled pipe in Fig. 1 shows the difference in bending deformation between fixed and rotating beams. A pipe with radius r and wall thickness h is bent by force P in the middle of the l-long span. If force P is directed along the *z*-axis (opposite to the axis), then the *y*-axis is the neutral one, and the bending deformation in section *A'A* at angle φ to the *y*-axis is equal to $\varepsilon = w''(x)r\sin\varphi$, where w'' is the second derivative of deflection $w(x)$ which coincides with the direction of *z*-axis, i.e. with the direction of P.

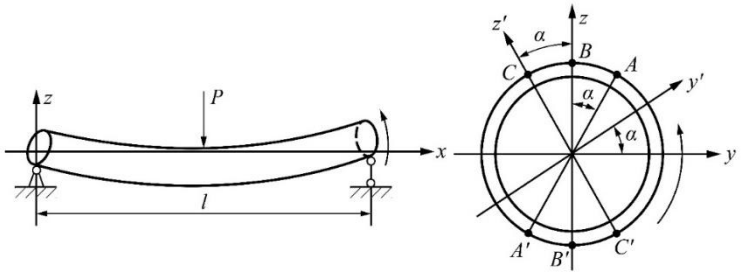

(a) (b)

Fig. 1. Bending deformation: (a) a fixed beam; (b) a rotating beam

The bending moment for the diagram shown in Fig. 1 (for $0 \leq x \leq 0.5l$) is $M_y = 0.5P_x$, and the moment of the *z*-axis is zero (since there are no forces in the direction of the *y*-axis). We used an approximate expression for curvature here, assuming that the first derivative is $|w'(x)| << 1$ [6–8]. Plastic deformation begins in sections *B* and *B'* and as we approach the section $x = 0.5l$ there are two zones of plastic deformation: those of compression *ABC* and tension *A'B'C'* where the stresses are $\sigma = -\sigma_m$ and $\sigma = +\sigma_m$ (where σ_m is the yield point). In zones *C'A* and *A'C*, elastic deformation occurs, and it is equal to $\sigma = E \cdot \varepsilon$ (where E is the elastic modulus).

Exploratory procedure

The resisting moment about the y-axis for fixed pipes in elastic-plastic deformation is equal to $M_y = 0.5\ P_x = \int_0^{2\pi} \sigma r^2 h \sin\varphi d\varphi$, the moment about the *z*-axis is $M_z = 0$. For some φ_1 characterizing the position of point *A* and *A'* $\sigma = Ew''r\sin\varphi = \pm\sigma_m$, and for $|\varphi| < \varphi_1$ deformations are elastic, and it are plastic for $\varphi_1 < \varphi < \pi - \varphi$ and $\pi - \varphi_1 < \varphi < 2\pi - \varphi_1$.

If the load acts in the *xz*-plane, Fig. 1(a), then for a fixed beam, the plastic zones *ABC* and *A'B'C'* are symmetrical with respect to the *z*-axis. When the pipe rotates and is under constant loads (the direction of rotation is shown in Fig. 1(b)), plastic deformations are possible only along arcs *AB* and *A'B'*, and after reaching the maximum (at point *B*) and the minimum (at point *B'*) deformations, unloading occurs in sections *BC* and *B'C'*.

However, if plastic deformations occur only under load along *AB* and *A'B'*, then the bending moment is $M_z \neq 0$, since the plastic zones are not symmetrical with respect to the *z*-axis. This contradicts the statement of the problem, since external loads act only in the *xz*-plane [9–11]. For a rotating pipe, the condition $M_z = 0$ can be fulfilled only if bending occurs not in the *xz*-plane, but in the *xz'*-plane, i.e. the deflection direction is parallel to the *z'*-axis (Fig. 1(b)) and forms the angle α with the *z*-axis. Then the maximum deformation is achieved at point *C*, the minimum one is at *C'* and unloading begins at these points. The neutral axis is also rotated by an angle α with respect to the *y*-axis.

Denoting the variable angle by φ, we define the bending stresses: $\sigma = \sigma_m$ for $\frac{\pi}{2} - \alpha < \varphi \leq \frac{\pi}{2} + \alpha$ (in *ABC*); $\sigma = \sigma_m - Ew''r[1 - \sin(\varphi - \alpha)]$ for $\frac{\pi}{2} + \alpha < \varphi \leq \frac{3}{2}\pi - \alpha$ (in the zone *CA'*); $\sigma = -\sigma_m$ for $\frac{3}{2}\pi - \alpha < \varphi \leq \frac{3}{2}\pi + \alpha$ (in the zone *A'B'C'*); $\sigma = -\sigma_m + Ew''r[1 + \sin(\varphi - \alpha)]$ for $\frac{3}{2}\pi + \alpha < \varphi \leq 0$, and for $0 < \varphi \leq \frac{\pi}{2} - \alpha$ (in the zone *C'A*).

For $\varphi = \frac{\pi}{2} - \alpha$ the stresses are $\sigma_m = -\sigma_m + Ew''r\left[1 + \sin\left(\frac{\pi}{2} - 2\alpha\right)\right]$ or $\frac{2\sigma_m}{Er} = w''(1 + \cos 2\alpha)$. Therefore, we get:

$$\frac{w''l}{a} = 1/\cos^2\alpha,\ a = \frac{\sigma_m l}{Er}. \tag{1}$$

The bending moment of the *y*-axis is $M_y(x) = \int_0^{2\pi} \sigma(\varphi)\, r^2 h \sin\varphi\, d\varphi$. With the calculations taken into account (1), we obtain a nonlinear bending equation:

$$M_y(x) = \pi\sigma_m r^2 h f(\alpha),\quad f(\alpha) = \frac{\pi - 2\alpha + \sin 2\alpha}{\pi\cos\alpha}. \tag{2}$$

For a pipe of length l loaded with concentrated force P (Fig. 1), the moment is $M_y(x) = 0.5Px$. Denoting $m = \frac{Pl}{4\pi\sigma_m r^2 h}$, we obtain in the zone of elastic-plastic deformation ($x_1 = \frac{0.5l}{m}$):

$$\frac{2mx}{l} = f(\alpha) \quad \text{for } x_1 < x \leq 0.5l, \tag{3}$$

and in the elastic zone:

$$w''(x) = \frac{2amx}{l^2} \quad \text{for } 0 \leq x \leq x_1. \tag{4}$$

If $m \leqslant 1.0$, then the deformations are elastic and $\alpha = 0$.

Since it follows from Eq. (1) that $\operatorname{tg}\alpha = \left(\frac{w''l}{a} - 1\right)^{0.5}$, then substituting α by w'' into Eq. (2), we obtain, instead of Eq. (3), the following equation:

$$x = lm^{-1}\varphi\left(\frac{w''l}{a}\right),\quad \varphi\left(\frac{w''l}{a}\right) = \frac{1}{\pi}\sqrt{\frac{w''l}{a}}\left[\pi + 2\sqrt{\frac{a}{w''l}\left(1 - \frac{a}{w''l}\right)} - 2\operatorname{arctg}\sqrt{\frac{w''l}{a} - 1}\right], \tag{5}$$

where φ is a differentiable function of w''. The greater is the load, the wider is the angle between the directions of force and deflection. As the load approaches it maximum, this angle tends to 90°. The value of $w'(x)$ in a parametric form in t function is:

$$x = \frac{l\varphi(t)}{2m},\ x_1 < x \leq 0.5l,\quad w'(x) = C_1 + \frac{a}{2m}\int_1^t t\frac{d\varphi}{dt}dt, \tag{6}$$

$$W(x) = C_2 + C_1 x + \frac{al}{4m^2}\int_1^t \frac{d\varphi(t)}{dt}\left[\int_1^t t\frac{d\varphi}{dt}dt\right]dt,$$

where C_1 and C_2 are the constants of integration.

The parameter t is then substituted into the function φ instead of the value $\frac{w''l}{a}$. The choice of the value $t = 1$ as the lower limit in the integrals of Eq. (6) corresponds to the boundary of the elastic-plastic and elastic zones ($\frac{w''l}{a} = 1.0$ when $x = x_1$). In the elastic zone, the solution of linear equation (4) under the condition $w = 0$ for $x = 0$ has the form:

$$w(x) = C_3 x + \frac{\frac{1}{3}amx^3}{l^2},\ 0 \le x \le x_1. \tag{7}$$

Based on the variability $w(x)$ and $w'(x)$ as well as $w' = 0$ for $x = 0.5l$ we define the constants $C_1 = -\frac{a}{2m}\int_1^{t_m} t\frac{d\varphi(t)}{dt}dt$, $C_2 = -\frac{al}{12m^2}$, $C_3 = C_1 - \frac{a}{4m}$, where t_m is the largest value of parameter t for $x = 0.5l$.

According to the first of Eqs. (6), we obtain $\varphi(t_m) = m$. Substituting constants into Eqs. (6) and integrating the double integral in parts, taking into account $\varphi(t_m) = m$, we define the maximum deflection w_m for $x = 0.5l$:

$$w_m = \frac{al}{12m^2}\left[1 + 3\int_1^{t_m} t\,\varphi(t)\frac{d\varphi(t)}{dt}dt\right],$$
$$\varphi(t) = \sqrt{t} + \frac{2}{\pi}\sqrt{t - \frac{1}{t}} - \frac{2\sqrt{t}}{\pi}\operatorname{arctg}\sqrt{t-1}. \tag{8}$$

By replacing variable t with $v(t)$, where v is a parameter similar to α and equal to $v = \operatorname{arctg}(t-1)^{\frac{1}{2}}$, we obtain $w_m = \frac{al}{12m^2}\left\{1 + \frac{3}{\pi^2}\int_0^{\alpha_m}\frac{1}{\cos^5 v}[(\pi - 2v)^2 + \sin^2 v]\sin v\,dv\right\}$, where α_m is the maximum value of angle α when $x = 0.5l$.

Having calculated the integral, we can define the maximum deflection as $w_m = \frac{al}{12m^2}\left[\frac{1}{4} + \frac{3(\pi-2\alpha_m)^2}{4\pi^3\cos\alpha_m} + \frac{3}{\pi^2}(\pi - 2\alpha_m)\left(\operatorname{tg}\alpha_m + \frac{1}{3}\operatorname{tg}^3\alpha_m - \frac{5}{\pi^2}\operatorname{tg}^2\alpha_m - \frac{16}{\pi^2}\ln\cos\alpha_m\right)\right]$, where value α_m is defined from the following equation:

$$f(\alpha_m) = \pi - 2\alpha_m + \sin\frac{2\alpha_m}{\pi\cos\alpha_m} = m, \tag{9}$$

where the parameter α_m is equal to the maximum angle between the directions of force and deflection (in the middle of the beam length).

Curves $\alpha_m(m)$ obtained by the numerical solution of Eq. (9) are shown in Fig. 2. With increasing m, parameter α_m increases and, when m approaches the limit value $m_0 = 1.275$, parameter $\alpha_m = 90°$, i.e., the direction of deflection when plastic deformation spreads over the entire section, deviates more and more from the direction of an external force and approaches the direction that makes up a right angle with the force.

Figure 3 shows the change in the value $\frac{w_m}{al} = w°$ (curve 1) and its projections on the z-axis (curve 2) and the y-axis (curve 3). The component of deflection in the direction of force P (along the z-axis) is not seen to increase with the onset of plastic deformation and the force increase, but to decrease. At m =1.16, the parameter $\alpha_m = 45°$ and the deflection projections on the z- and y-axes are equal. In elastic deformation, when the stresses are completely specified by deformations, rotation does not affect the beam bending. However, in elastic-plastic deformation, when the stresses depend on the loading history, the beam rotation significantly changes the bending process and leads to the lateral displacement and deviation of the deflection from the force plane [5,9,12]. Since angle α

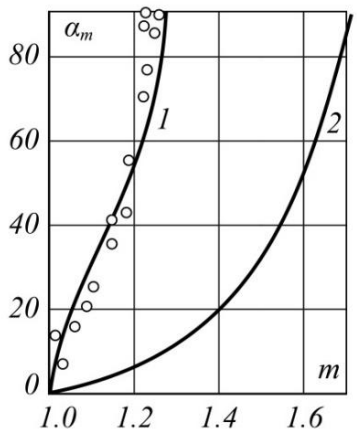

Fig. 2. Curve $\alpha_m(m)$ obtained by numerical solution of Eq. (9), (curve 1)

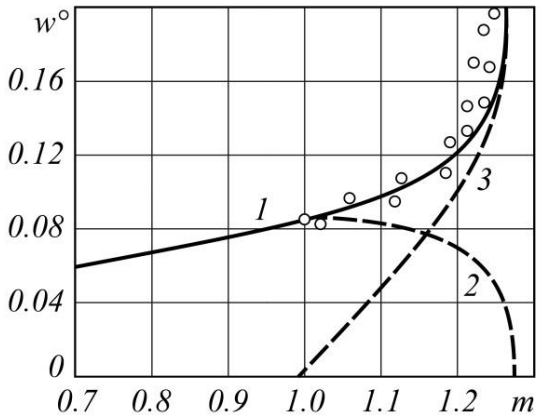

Fig. 3. Graphs of the value $\frac{w_m}{al} = w^\circ$ (curve 1) and its projections on the *z*-axis (curve 2) and the *y*-axis (curve 3)

depends on the bending moment and the *x* coordinate, the beam axis is not flat, but a space curve.

Results and Discussion

The problem is considered for the case where the bending moment vector rotates around the pipe axis, and the deflection direction rotates at the same speed, with a phase shift of angle α.

To estimate the range of bending parameters, we can neglect tangential torsional stresses τ. If we assume that for each revolution of the pipe, the work equal to $4\sigma_m^2\left(\frac{w''l}{a-1}\right)/E$ contributes to plastic deformation of a unit volume, and the entire volume of the pipe with length $(l - 2x_1)$ undergoes plastic deformation, then we obtain an upper bound of the plastic work as follows $A = \frac{8\sigma_m^2}{E}\pi rlh\left(1-\frac{1}{m}\right)\left(\frac{w''l}{a}-1\right) = 4\pi\tau r^2 h$. Therefore, we have $\frac{\tau}{\sigma_m} = \frac{2a}{\pi}\left(1-\frac{1}{m}\right)\left(\frac{w''l}{a}-1\right)$. Assuming the maximum value of $m_0 = 1.275$, we find that $\frac{\tau}{\sigma_т} = 0.137a\left(\frac{w''l}{a}-1\right) = 0.137a\,\mathrm{tg}^2\,\alpha_m$.

Assuming that the condition $\frac{\tau}{\sigma_m} < 0.05$ must be met, then, if $x = 0.5l$, it is sufficient that $w''l < 0.362 - a$, $\mathrm{tg}\,\alpha_m < \left(\frac{0.362}{a}\right)^{0.5}$. For example, for $\sigma_m = 240$ MPa, $E = 2{\cdot}10^5$ MPa, $\frac{l}{r} = 10$, $a = 1.2{\cdot}10^2$, $\mathrm{tg}\,\alpha_m < 5.5$, $\alpha_m < 79.5°$, i.e., the formulas are applicable for large values of α_m [11,13–16]. Note that the influence of tangential stresses on a pipe can be approximately accounted for by substituting $\sigma_1 = (\sigma_m^2 - 3\tau^2)^{0.5}$ into the equations instead of σ_m.

For other loading schemes, Eq. (2) is solved for *x*, and Eqs. (6) and (7), $\varphi(t_m) = m$ is true if the corresponding $\varphi(t)$ function is defined. For example, for a cantilevered pipe of length *l*, loaded with force *P* we have $\varphi(t) = 2\left[m - \sqrt{t} - \frac{2}{\pi}\sqrt{1-\frac{1}{t}} - \frac{2}{\pi}\mathrm{arctg}\sqrt{t-1}\right]$, $m = \frac{Pl}{\pi\sigma_m r^2 h}$. For a pipe supported on two points, loaded with a uniform distributed load of intensity *p*, we have, for $m = \frac{pl^2}{8\pi\sigma_m r^2 h}$: $\varphi(t) = m + \left\{m\left[m - \sqrt{t} - \frac{2}{\pi}\sqrt{1-\frac{1}{t}} - \frac{2}{\pi}\mathrm{arctg}\sqrt{t-1}\right]\right\}^{\frac{1}{2}}$.

Many problems that are important for practical applications lead to the equations similar to Eq. (2), which, with a complex dependence on the variable w'', are solved with respect to the variable x in a form similar to Eq. (3). Equations (6) then determine the solution for known values m and $\varphi(t)$, showing the advantage of the parametric method to solve problems of elastic-plastic bending [17–22].

The deformation of a free pipe is discussed above. If the deflection plane is fixed in the xz-plane, $\alpha = 0$ can be ensured by using rigid, smooth rulers that hold the beam along its entire length to prevent lateral displacement. In this case, $M_y(x) = \frac{\sigma_m r^2 h(2\pi - 2\alpha_1 + \sin 2\alpha_1)}{1+\cos\alpha_1}$, $M_z(x) = 4\pi\sigma_m r^2 h\left(1 - \frac{a}{w''l}\right)$, $\alpha_1 = arccos(2a-1)$.

The rulers apply pressure to the pipe, creating this value $M_z(x)$. As force P increases, moment M_y reaches its maximum at the angle of $\alpha_1 = 57°$, $m_0 = 1.075$. After that, it decreases, while the moment M_z continues to increase. Therefore, the maximum load limit is not defined by $m_0 = 1.275$, as it would be with a free beam, but by $m_0 = 1.075$, which is 18 % less.

Let's consider the bending of thick-walled circular beams with outer and inner radii r and r_1. There can be two cases (Fig. 4): in the first one, plastic deformation does not penetrate the entire thickness of the beam and deformations are elastic for $\rho \leqslant \rho_0$, Fig. 4(a). In this case, stresses are $\sigma = Ew''\rho\sin(\varphi - \alpha)$. Bending occurs on the z'-axis, and the neutral axis y' has zero deformation. Plastic zones ABC and $A'B'C'$ are shown shaded in Fig. 4. The equation of the line AC has the form $\rho_1 = \frac{2ar}{[w''l[1+\sin(\varphi-\alpha)]]}$, and the equation of the line $A'C'$ is $\rho_2 = \frac{2ar}{[w''l[1-\sin(\varphi-\alpha)]]}$. For $\varphi = \frac{\pi}{2} + \alpha$ (point C) and $\varphi = \frac{3\pi}{2} + \alpha$ (point C') $\rho_1 = \rho_2 = \rho_0 = ur$; $u = \frac{a}{w''l}$.

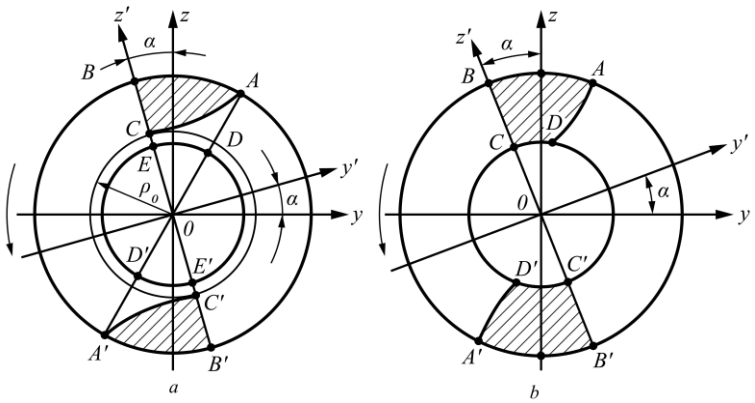

Fig. 4. Bending schemes of thick-walled circular beams with external and internal radii r and r_1:
(a) plastic deformation does not penetrate the entire thickness of the beam;
(b) plastic deformation penetrates the entire thickness of the beam

The scheme shown in Fig. 4(a), can be used for $\rho_0 \geqslant r_1$ or $u \geqslant 2u_1$, $u_1 = \frac{0.5r}{r_1}$. Unloading happens in zones $BCA'C'$ and $B'C'CA$. The bending moments about the y- and z-axes are equal to $M_y(x) = \iint \sigma(\rho,\varphi)\,\rho^2 \sin\varphi\, d\rho d\varphi$; $M_z(x) = \iint \sigma(\rho,\varphi)\,\rho^2 \cos\varphi\, d\rho d\varphi$, where integrals are calculated over the entire contour of the section. According to the calculations, we obtain:

$$M_y(x) = \sigma_m r^3[f_1(u)\sin\alpha + f_2(u)\cos\alpha],$$
$$M_z(x) = \sigma_m r^3[f_3(u)\sin\alpha + f_4(u)\cos\alpha], \quad (10)$$

$$f_1(u) = f_4(u) = \frac{4}{3} - 2u + \frac{2}{3}u^3,$$
$$f_2(u) = -f_3(u) = \frac{\pi}{8u} + \frac{1}{4u}\arcsin(2u-1) - \frac{4\pi u_1^4}{u} + \sqrt{u(1-u)}\left(\frac{9}{5} - \frac{1}{2u} - \frac{4}{15}u - \frac{8}{15}u^2\right). \quad (11)$$

If $M_z(x) = 0$, then $\operatorname{tg}\alpha = \frac{f_1(u)}{f_2(u)}$; excluding value α from Eq. (10), we obtain the bending equation:

$$\frac{M_y(x)}{\sigma_m r^3} = \sqrt{f_1^2(u) + f_2^2(u)}. \tag{12}$$

For a beam loaded with concentrated force P, Eq. (6) can be applied by taking function $\varphi(t)$ as:

$$\varphi(t) = c\sqrt[4]{f_1^2\left(\frac{1}{t}\right) + f_2^2\left(\frac{1}{t}\right)},$$
$$c = \frac{}{[\pi(1-16u_1^4)]}, \tag{13}$$

and constant $m = \frac{Pl}{[\pi\sigma_m r^3(1-16u_1^4)]}$. In the special case, when $u_1 = 0$ we have a solid circular shaft.

The linear equation (4) works in the elastic zone. The maximum deflection is defined by Eq. (8), into which function $\varphi(t)$ should be substituted according to Eq. (13). If $u_m = \frac{1}{t_m} < 2u_1$, then the scheme shown in Fig. 4(b), takes place, i.e. plastic deformation will spread along the entire section of the beam. Plastic deformation occurs in shaded areas *ABCD* and *A'B'C'D'*, and unloading occurs in zones *BCD'A'* and *B'C'DA*. According to the calculations similar to Eqs. (10), we obtain:

$$M_y(x) = \sigma_m r^3[f_5(u)\sin\alpha + f_6(u)\cos\alpha],$$
$$M_z(x) = \sigma_m r^3[f_7(u)\sin\alpha + f_8(u)\cos\alpha],$$
$$f_5(u) = f_8(u) = \frac{4}{3} - 2u + 8uu_1^2 - \frac{32}{3}u_1^3,$$
$$f_6(u) = -f_7(u) = \frac{\pi}{8u} + \frac{1}{4u}\arcsin(2u-1) - \frac{4u_1^4}{u}\arcsin\left(\frac{u}{u_1} - 1\right) - 2\pi u_1^4 +$$
$$+\sqrt{u(1-u)}\left(\frac{9}{5} - \frac{1}{2u} - \frac{4}{15}u - \frac{8}{15}u^2\right) + \sqrt{\frac{u}{u_1}\left(2 - \frac{u}{u_1}\right)}\left(4\frac{u_1^4}{u} - \frac{36}{5}u_1^3 + \frac{8}{15}uu_1^2\right). \tag{14}$$

For $u = u_1$ from Eqs. (11) and (14) we have $f_1(u_1) = f_5(u_1)$, $f_2(u_1) = f_6(u_1)$. In the special case, if $M_z = 0$, then $\operatorname{tg}\alpha = \frac{f_5(u)}{f_6(u)}$. In Eqs. (8), instead of $\varphi(t)$ for $0 \leqslant u \leqslant 2u_1$, we substitute:

$$\varphi_1(t) = c\left[f_5^2\left(\frac{1}{t}\right) + f_6^2\left(\frac{1}{t}\right)\right]^{0.5}. \tag{15}$$

When considering the bending of a beam in the elastic zone for $0 \leqslant x \leqslant x_1$, we have Eq. (4), then for $x_1 < x \leqslant x_2$ there will be a zone of elastic-plastic deformation in which there is an elastic core in the beam section (Fig. 4(a)) and Eq. (11) $x_2 = \frac{0.5l\varphi\left(\frac{1}{u_1}\right)}{m}$ is valid.

For $x_2 < x \leqslant 0.5l$ there is a zone of elastic-plastic deformation where the plastic flow spreads over the entire thickness (Fig. 4(b)) and Eq. (14) is valid. Solving the bending equations, we find the maximum deflection:

$$w_m = \frac{al}{12m^2}\left[1 + 3\int_1^{2t_1} f\,\varphi(t)\frac{d\varphi(t)}{dt}dt + 3\int_{2t_1}^{t_m} f\,\varphi_1(t)\frac{d\varphi_1(t)}{dt}dt\right],\ t_1 = \frac{1}{u_1}, \tag{16}$$

where value t_m is defined by equation $\varphi_1(t_m) = m$. The equations obtained should be applied if $0 \leqslant u_m < 2u_1$; in the case of $2u_1 \leqslant u_m \leqslant 1.0$, the equation $\varphi(t_m) = m$ and Eq. (8) are valid, where $\varphi(t)$ is defined by Eq. (13).

Based on numerical calculations performed with these equations, values $\alpha_m(m)$ and $w°(m)$ shown in Fig. 2 (curve 2) and Fig. 5 [16–21,23–30] were determined. Note that the dependencies $w_m(m)$ are satisfactorily defined by equation $w_m = \frac{1}{12}al\left[\frac{m_0-1}{m_0-m}\right]^{\frac{1}{3}}$, where the limiting moment is $m_0 = \frac{16(1-8u_1^3)}{3\pi(1-16u_1^4)}$.

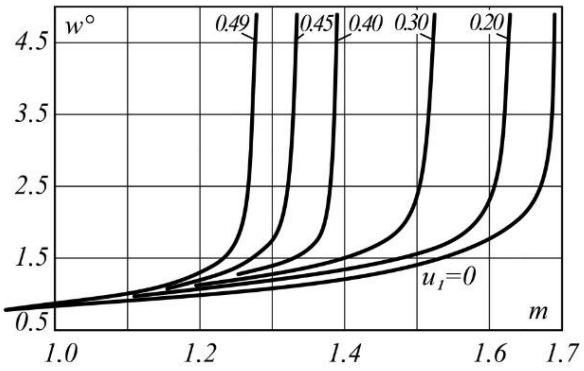

Fig. 5. Graphs of values $\alpha_m(m)$, $w°(m)$

The experimental study was performed in bending copper and aluminum pipes with radius 0.6 and 1.0 cm and thickness 0.1 and 0.2 cm. The installation was mounted on a lathe. The pipes were rotated with a lathe chuck, and the force was applied by a clip with gaskets that reduce the crumpling of the hollow blank through a lathe caliper with an elastic dynamometer. Deflection angle α_m was determined by the deflection components.

The experimental points are shown in Figs. 2 and 3. For $1.0 \leqslant m \leqslant 1.20$, the experimental data are in satisfactory agreement with the calculated ones; the discrepancies do not exceed 20 % for both angle α_m and deflection value. For $m > 1.20$, the discrepancy between the calculated and experimental values increases.

In all cases when rotating pipes are bent and plastic deformation happens, lateral displacement occurs. When bearing capacity is lost and deformation decreases, the deflection of pipes occurs not in the direction of force action, as for fixed beams, but at angle 90° to the force action line.

Conclusions

1. The elastic-plastic deformation of rotating circular blanks differs from that of fixed pipes significantly. In this case, the direction of maximum deflection does not coincide with the direction of the bending force.
2. Graphs and analytical dependences of deflection on load with respect to bending force are given. It is shown that the deflection of a rotating blank (pipe) can exceed that of a stationary one by 20–25 %. As the maximum load approaches, deflection occurs at an angle of ~ 90° to the force direction.
3. At the stage of unloading, or deformation reduction, it is necessary to carry out symmetrical tension-compression cycles, which ensures the quality of straightening.
4. The design of proper machine tools must take into account the movement of the blank.

CRediT authorship contribution statement

Tatyana V. Brovman : writing – original draft.

Conflict of interest

The author declares that she has no conflict of interest.

References

1. Shelest AE, Yusupov VS, Rogachev SO, Andreev VA, Karelin RD, Perkas MM. Study of the additional possibility of the effect of elastic-plastic alternating deformation on the properties of metal materials during their processing on a roller straightening machine. *Metally.* 2023;1: 75–83. (In Russian)
2. Shelest AE, Yusupov VS, Perkas MM, Sheftel' EN, Akopyan KE, Prosvirnin VV. Formation of the Mechanical Properties of Copper Strips during Alternating Elastoplastic Bending. *Russian Metallurgy (Metally).* 2018;2018: 500–506.
3. Shatalov RL, Genkin AL. Sheet mill control in steel strip hot rolling. *Journal of Chemical Technology and Metallurgy.* 2015;50(6): 624–628.
4. Ivlev DD. *Theory of ideal plasticity.* Moscow: Nauka; 1966. (In Russian)
5. Rudskoi AI, Kodzhaspirov GE, Kamelin EI Simulation of dynamic recrystallization of austenitic corrosion-resistant steel during the formation of a complex section by high-temperature thermomechanical treatment. *Russian Metallurgy (Metally).* 2022;2022: 1181–1185.
6. Brovman TV. Elastic-plastic bending deformation during profiling. *Ferrous metallurgy. Izvestiya VUZov.* 2000;9: 36–39. (In Russian)
7. Shapiro GS. On the limiting and elastic-plastic state of structures. *Izv. of the USSR Academy of Sciences. Mechanics and Mechanical Engineering.* 1963;4: 138–144. (In Russian)
8. Klyushnikov VD. *Mathematical theory of plasticity.* Moscow: Publishing House of Moscow State University; 1979. (In Russian)
9. Brovman TV. Forces in case of local deformation of tubular billets. *Technology of Metals.* 2015;6: 9–13. (In Russian)
10. Savikovskii AV, Semenov AS. Influence of material anisotropy on the interaction between cracks under tension and shear. *Materials Physics and Mechanics.* 2023;51(5): 24–37.
11. Gulin AE, Korchunov AG, Konstantinov DV, Sheksheev MA, Polyakova M. Features of the properties of steel with the trip effect under various types of deformation loading. *Materials Physics and Mechanics.* 2023;51(5): 152–164.
12. Fomin SV, Rostovtsev VS, Meltsov VU, Shirokova ES. Prediction of mechanical properties of elastomeric materials using neural networks. *Materials Physics and Mechanics.* 2023;51(5): 66–78.
13. Brovman TV, Kutuzov AA. Improving accuracy in the manufacture of curved metal workpieces by bending deformation. *Russian Metallurgy (Metally).* 2016;2016: 477–484.
14. Andrianov IK, Feoktistov SI. Integral equations of deformation of cylindrical workpieces in axisymmetric matrices of complex shape. *Materials Physics and Mechanics.* 2023;51(2): 112–121.
15. Brovman TV. Nonstationary process plastic deformation in bending of workpieces. *The Scientific Heritage.* 2019;36: 55–59. (In Russian)
16. Babeshko VA, Evdokimova OV, Babeshko OM. On the exact solution of mixed problems for multicomponent multilayer materials. *Materials Physics and Mechanics.* 2023;51(5): 1–8.
17. Rudskoy AI Kojaspirov GE, Kliber Ch, Apostolopoulos A, Kitaeva DA. Physical fundamentals of thermomechanical processing in ultrafine-grained metallic materials manufacturing. *Materials Physics and Mechanics.* 2020;43(1): 51–58.
18. Prokofieva OV, Beigelzimer YaE, Usov VV, Shkatulyak NM, Savkova TS, Sapronov AN, Prilepo DV, Varyukhin VN. Formation of a Gradient Structure in a Material by Twist Extrusion. *Russian Metallurgy (Metally).* 2020;2020: 573–578.
19. Khvan AD, Khvan DV, Voropaev AA. Bauschinger Effect during the Plastic Forming of Ferrous Metals. *Russian Metallurgy (Metally).* 2021;3: 81–84.
20. Bakulin VN. Block based finite element model for layer analysis of stress strain state of three-layered shells with irregular structure. *Mechanics of Solids.* 2018;53: 411–417.
21. Maksimov EA, Shatalov RL, Shalamov VG. Calculation of Residual Stress and Parameters of Sheet Springing on a Roller Leveler. *Steel in Translation.* 2021;51: 1–6.
22. Brovman TV. Analysis of Plastic Deformation by the Method of Inverse Problems. *Inorganic Materials: Applied Research.* 2025;16(3): 724-729.
23. Brovman TV. Obtaining accurate parts in non-stationary processes of bending deformation. *Physics and Chemistry of Materials Treatment.* 2020;2: 80–84. (In Russian)
24. Maximov EA, Ustinovsky EP. Method for calculating force in the machine applied for correcting the "ski formation" defect of plates. *Mechanical Equipment of Metallurgical Plants.* 2019;2(13):45–48. (In Russian)
25. Zaides SA, Hai NH. Influence of tool geometry on the stress-strain state of cylindrical parts during reversible surface plastic deformation. *Russian Engineering Research.* 2023;43: 1088–1094.

26. Shalaevsky DL. Investigation of thermal mode of hot-rolling mill working rolls in order to improve the accuracy of calculating the thermal profile of their barrels' surface. *Izvestiya Ferrous Metallurgy.* 2023;66(3): 283–289.
27. Nikolaev VA, Roberov IG. Calculation of roll deflection, taking into account nonuninformity of linear contact forces. *Proizvodstvo Prokata.* 2019;12: 9–14. (In Russian)
28. Pimenov VA, Lagman AI, Kovalev DA. Analysis and Mathematical Simulation of Formation Regularities of Strip Transversal Profile during Hot Rolling. *Steel in Translation.* 2020;50: 107–111.
29. Kukhar VD, Korotkov VA, Yakovlev SS, Shishkina AA. Formation of a mesh of spiral wedge rotrusions on the inner surface of a steel shell by local plastic deformation. *Chernye Metally.* 2021;65: 65–68.
30. Zakarlyuka SV, Rudenko EA, Goncharov VE. Elastic tension of non-planar strips with asymmetric out-of-flatness for the biquadratic law of stress distribution over the width. *Metallurgist.* 2024;68: 239–247.